



저작자표시-비영리-변경금지 2.0 대한민국

이용자는 아래의 조건을 따르는 경우에 한하여 자유롭게

- 이 저작물을 복제, 배포, 전송, 전시, 공연 및 방송할 수 있습니다.

다음과 같은 조건을 따라야 합니다:



저작자표시. 귀하는 원저작자를 표시하여야 합니다.



비영리. 귀하는 이 저작물을 영리 목적으로 이용할 수 없습니다.



변경금지. 귀하는 이 저작물을 개작, 변형 또는 가공할 수 없습니다.

- 귀하는, 이 저작물의 재이용이나 배포의 경우, 이 저작물에 적용된 이용허락조건을 명확하게 나타내어야 합니다.
- 저작권자로부터 별도의 허가를 받으면 이러한 조건들은 적용되지 않습니다.

저작권법에 따른 이용자의 권리는 위의 내용에 의하여 영향을 받지 않습니다.

이것은 [이용허락규약\(Legal Code\)](#)을 이해하기 쉽게 요약한 것입니다.

[Disclaimer](#)

수의학석사 학위논문

**Efficacy of 3D-printed allogenic  
biomaterial implant for the  
regeneration of knee articular cartilage  
in canine trochlear block recession  
models**

개의 활차 블록 절제 모델에서 관절 재생을 위한  
3D 프린터로 제작된 동종유래 생체재료 이식의  
효과 연구

2023년 02월

서울대학교 대학원  
수의학과 임상수의학 전공  
이 한 솔

# **Efficacy of 3D-printed allogenic biomaterial implant for the regeneration of knee articular cartilage in canine trochlear block recession models**

개의 활차 블록 절제 모델에서 관절 재생을 위한 3D 프린터로 제작된 동종유래 생체재료 이식의 효과 연구

지도교수 김 민 수

이 논문을 수의학석사 학위논문으로 제출함

2022년 10월

서울대학교 대학원

수의학과 임상수의학 전공

이 한 솔

이한솔의 석사학위논문을 인준함

2022년 12월

위 원 장	_____	(인)
부 위 원 장	_____	(인)
위 원	_____	(인)

# **Abstract**

## **Efficacy of 3D-printed allogenic biomaterial implant for the regeneration of knee articular cartilage in canine trochlear block recession models**

Hansol Lee

Veterinary Clinical Sciences Major

Graduate School of Veterinary Medicine

Seoul National University

The purpose of this study was to confirm the inflammatory alleviation and therapeutic effect of 3D printed biomaterial containing lyophilized costal cartilage matrix (LCCM), micronized adipose tissue (MAT), and fibrin glue. This study used the canine trochlear block recession model. The control group performed only trochlear block recession and the experimental groups were classified into LCCM + MAT + fibrin glue, LCCM + fibrin glue, only fibrin glue, and syringe type groups according to the composition of the biomaterial implant. To prove the therapeutic effect, magnetic resonance imaging (MRI), an enzyme-linked immunosorbent assay (ELISA) of the synovial fluid, and histopathological examination were performed. In the synovial joint ELISA, we confirmed the decreased matrix metalloproteinase-3 (MMP-3) level and increased tissue inhibitor of metalloprotease-1 (TIMP-1) level tendency in the LCCM + MAT + fibrin glue group. In addition, MRI analysis confirmed that the amount of joint fluid increased in the control group compared to the LCCM + MAT + fibrin glue group. Therefore,

the LCCM + MAT + fibrin glue group considered that joint inflammation and the joint fluid due to arthritis were less than in other groups. In the histopathological examination, the LCCM + MAT + fibrin glue group compared to other groups showed integrity between normal tissue and lesion area, the number of chondrocytes, and regeneration of hyaline cartilage. We confirmed that the treatment of cartilage lesions was effective in the LCCM + MAT + fibrin glue group. In the canine cartilage lesion experimentally induced, we confirmed that 3D-printed LCCM + MAT + fibrin glue biomatrix has a significant effect on cartilage lesion repair, regeneration, and inflammation reduction.

---

**Keywords:** articular cartilage, 3D printed implant, regeneration, canine knee, trochlear block recession

**Student Number:** 2020-28574

# Table of Contents

<b>Introduction .....</b>	<b>1</b>
<b>Materials and Methods .....</b>	<b>4</b>
1. Experimental Animals .....	4
2. Study Design .....	4
3. Preparation of Biomaterial Inks and Fabrication of 3D-printed Bio-scaffold .....	6
4. Preparation of Experimental Surgery .....	7
5. Surgery Procedure .....	7
6. Analysis .....	8
7. Statistical Analysis.....	9
<b>Results.....</b>	<b>10</b>
1. Gross Appearance .....	10
2. Serum Level of Matrix Metalloproteinases-3 (MMP-3) and Tissue Inhibitors of Matrix Metalloproteinases-1 (TIMP-1).....	12
3. Magnetic Resonance Imaging (MRI) Analysis .....	14
4. Microscopic findings .....	16
<b>Discussion .....</b>	<b>22</b>
<b>Conclusion .....</b>	<b>26</b>
<b>References.....</b>	<b>27</b>
<b>Abstract in Korean .....</b>	<b>32</b>

# Introduction

In small dogs, the early grade of patellar luxation can be managed by conservative treatment. However, as stages 2 and 3 progress, the patella slides over the articular cartilage groove, causing progressive cartilage erosion on the patella and trochlear surface, and/or cranial cruciate ligament disease and rupture. Untreated patellar luxation increases the incidence of degenerative joint disease (DJD) and if it progresses to over stage 3, surgical treatment such as sulcoplasty, and metal implantation is inevitable, but osteoarthritis is frequently caused by risk factors such as implant reaction, infection, and inflammation (di Dona et al., 2018; DiVincenzo et al., 2017; Dokic et al., 2015; Romesburg et al., 2010). In large dogs, surgical treatment such as femoral corrective osteotomy is inevitable in most cases (Spencer Johnston et al., n.d.). In the case of patellar luxation, the damaged cartilage area is repaired by mixed fibrocartilage rather than hyaline cartilage, which is lacking biomechanical characteristics and is weaker in structure and function than hyaline cartilage, gradually increasing the occurrence of degenerative joint disease (DJD) (Armiento et al., 2019; Falah et al., 2010; Knutsen et al., 2004; Yoon et al., 2015).

The cartilage lesion healing is challenging due to its atypical avascular, aneural, alymphatic, and hypocellular environment. Not properly repaired cartilage lesion causes pain, edema, and decreased motility, eventually leading to osteoarthritis and complication such as cruciate ligament damage and fractures. These naturally occurring OA have similarities between dogs and humans and share a basic pathological process (Armiento et al., 2019; Falah et al., 2010; Knutsen et al.,

2004; Yoon et al., 2015).

Internal medical treatment for early cartilage damage can be performed, but nonsteroidal anti-inflammatory drugs (NSAIDs) do not reach the depth level of cartilage, and the component of the cartilage extracellular matrix such as glucosamine and chondroitin have slow acting, and evidence on the effectiveness is lacking. Minimally invasive injective treatment glucocorticoid or viscosupplementation such as hyaluronic acid can be applied, but only temporarily reduce pain and there is no proven disease-modifying therapy available. Surgical approaches can be divided into reparative and regenerative techniques. Among reparative options, bone marrow stimulation procedures are commonly applied but the repair tissue response can be unpredictable. Patients should adjust their level of activity in consideration of the strength and function of the treated cartilage. Regenerative techniques aim at the newly grown tissue restoring a normal joint by the production of hyaline-like cartilage that is mechanically and functionally stable (Marcacci et al., 2013). But, many current regenerative techniques such as autologous chondrocyte implantation (ACI), osteochondral transplantation, and allograft implants usually do not produce fully normal mechanical strength, and integrity and may also have additional surgical risk (Sutherland et al., 2015).

Therefore, the tissue engineering field has recently seen an emerging trend toward acellular biomaterials applied together or alternative to cell-based therapies (Sutherland et al., 2015). In addition to the source of cells, it is important to provide a suitable scaffold and micro-environment to conducive cell growth and differentiation in tissue regeneration therapy. When a three-dimensional printer is applied, different biomaterials and biocompatible bioinks are constructed for

suitable position and placement of cells and biomaterials through a layer-by-layer addition to enable complex optimized tissue engineering (Dzobo et al., 2019; Ryu et al., 2022).

In addition, dogs are suitable as a laboratory and clinical model of the cartilage repair study in that they can be applied reliably in human-type postoperative management such as bandaging, splint, walking, or training on treadmills and antemortem diagnostic monitoring protocol containing gait and kinematic analysis, MRI (Journal, 1988; Sasaki et al., 2019). Previous studies used biomaterials derived from autologous but were conducted by applying the manual dispensing method rather than 3D printing, so this study was conducted to compare the therapeutic differences between 3D printed and manual dispensing method (Escobar Ivirico et al., 2017). Ryu et al. demonstrated that three-dimensional printed biomaterials derived from xenogenic human origin could repair osteochondral lesions in canine osteochondral defect models. In this study, biomaterials derived from allogenic canine origin was used and applied to the canine trochlear block recession model (Ryu et al., 2022).

We hypothesized that biomaterials, including LCCM and MAT produced by 3D printing, could promote optimized inflammation reduction and cartilage regeneration. The purpose of this study is to investigate the inflammatory alleviation and therapeutic effects of 3D printed biomatrix application of allografted lyophilized costal cartilage matrix (LCCM), micronized adipose tissue (MAT), and fibrin glue using a canine trochlear block recession model.

# Materials and Methods

## 1. Experimental Animals

We used 8 Beagle dogs (male, 12-month-old) average weighed around 10 kg. Before the experiment, all dogs were tested for physical examination, blood analysis, radiography, gait, and orthopedic palpation test. Finally, there was no risk factor, and it was confirmed to be healthy beagle dogs.

## 2. Study Design

Clinical follow-up procedures were continued by week 32 from the day of experimental surgeries and then euthanized. In this study, a total of 8 dogs were used. Each leg of the dogs was considered as one model, and 15 models were set excluding one leg that was not assigned among the 16 legs. We divided models into one control group and four experimental groups. The control group performed only trochlear block recession and the experimental groups were classified into LCCM + MAT + fibrin glue, LCCM + fibrin glue, only fibrin glue, and syringe type groups according to the composition of the biomaterial implant. (**Table 1**) The syringe injection group was assigned to evaluate the effect of 3D printing under the same composites. All experimental procedures were ethically cleared by Institutional Animal Care and Use Committee at Seoul National University (IACUC-SNU-210127-4-4)

**Table 1.** The composition of the 3D printed biomatrix for canine trochlear block recession models.

Group	Dogs	Left	Right
Negative	#1	Block recession*	Block recession*
Control	#2	N/A**	Block recession*
Experimental Groups	#3	LCCM + MAT + fibrin glue (3D printed)	LCCM + MAT + fibrin glue (3D printed)
	#4	LCCM + MAT + fibrin glue (3D printed)	LCCM + fibrin glue (3D printed)
	#5	LCCM + fibrin glue (3D printed)	LCCM + fibrin glue (3D printed)
	#6	Fibrin glue (3D printed)	Fibrin glue (3D printed)
	#7	Fibrin glue (3D printed)	Syringe injection***
	#8	Syringe injection***	Syringe injection***

\* Designated as negative control, \*\* Not assigned, \*\*\* LCCM+ MAT mixtures were intra-articularly injected after sulcoplasty

### **3. Preparation of Biomaterial Inks and Fabrication of 3D-printed Bio-scaffold (BS)**

#### **3.1. Micronized Adipose Tissue (MAT)**

Canine subcutaneous adipose tissues were obtained from each dog's abdomen site right before sulcoplasty. The tissues were mechanically minced with Metzenbaum scissors for a minute and then micronized with 2000, 1000, 400, and 200  $\mu\text{m}$  Adinizer filter system (BSL Rest, Seoul, Republic of Korea). 10 mL of micronized tissues were collected from each dog and the oily supernatant was discarded.

#### **3.2. Allografted Lyophilized Costal Cartilage Matrix (LCCM)**

The canine costal cartilages were prepared into white powder form (LCCM) by lyophilization (ROKIT Healthcare, Seoul, Republic of Korea) and ball milling procedure with an average particle size between 100-200  $\mu\text{m}$ . The LCCM powder was distributed into 3 mL BD<sup>®</sup> Luer-Lock syringe (BD, NJ, USA) equally for 50 mg. The samples were then sterilized with gamma radiation process.

#### **3.3. Fabrication of 3D-printed Bio-scaffold (BS)**

Fabrication of 3D-printed BS was performed using Dr. INVIVO 3D bioprinter (ROKIT Healthcare, Seoul, Republic of Korea). The detailed procedure is described in our previous article

#### **4. Preparation of Experimental Surgery**

All animals were fasted for 12 hours before the experimental procedures to prevent vomiting and aspiration due to general anesthesia. 22 mg/kg cefazolin as preventive antibiotics, 3 mg/kg tramadol as analgesics, and 1mg/kg maropitant citrate (Cerenia®) for preventing aspiration pneumonia caused by vomiting were intravenously injected 30 minutes before the surgery. Then the dogs were sedated with 20 ug/kg medetomidine (Domitor®) IM and induced with 2 mg/kg alfaxalone IV. The anesthesia was maintained with 2-3% isoflurane. All surgical sites were shaved and aseptically prepared.

#### **5. Surgery Procedure**

After the preparation of general anesthesia, we approached medially the stifle joints incising craniomedially over the patella. All dogs received trochlear block recession sulcoplasty. A fine-toothed, handheld patella saw was used to make the cuts in trochlear regions. Each abaxial osteotomy is angled approximately 10 degrees axially toward the sagittal plane of the femur. We use a #15 blade to elevate osteochondral blocks from the patellar groove. The osteochondral block was undermined from proximal and distal margins to meet in the center of the block. Except for negative control, other groups had bone removed from the bottom of the incised block to deepen the sulcus. The basilar surface of the osteochondral block was resected with a rongeur. The proximal and/or ends of the osteochondral block were trimmed to match the shape of the recipient bed. The osteochondral block is placed in the recipient bed. Then, the bio-scaffold was implanted on the replaced osteochondral blocks. The retinaculum and joint capsule

were sutured with 3-0 PDS surgical sutures (Ethicon, Raritan, NJ, USA) and the skin incision was closed using surgical staplers (Covidien, Dublin, Ireland).

## **6. Analysis**

### **6.1 Enzyme-linked Immunosorbent Assay (ELISA) of the Synovial Fluid**

The synovial fluid samples were drained from knee joints using 23 gauge needles at 2, 4, and 8 months after surgery. The samples were immediately stored in a deep freezer (-80°C) until use. The samples were diluted 50X with normal saline and analyzed with Canine Matrix Metalloproteinase 3 ELISA Kit (MBS043123, MyBioSource, San Diego, CA, USA) and Canine Tissue Inhibitors of Metalloproteinase 1 (TIMP1) ELISA Kit (MBS455046, MyBioSources, San Diego, CA, USA) according to the manufacturer's instructions. The 450 nm absorbance was measured with TECAN Sunrise Microplate Reader (Tecan, Männedorf, Switzerland).

### **6.2 Histopathology of Hematoxylin and Eosin (H&E), Alcian Blue Staining**

The histopathologic samples were obtained by euthanizing the experimental dogs 8 months after surgery. All samples were rinsed using phosphate-buffered saline (PBS) and fixed using 10% neutral buffered formalin at 25-30°C. After decalcification in 15% ethylenediamine-tetra acetic acid (EDTA) (pH 7.2-7.4), samples were dehydrated with multi-series

of ethanol and embedded in paraffin and sectioned into 5  $\mu\text{m}$  slides. Samples were stained with hematoxylin and eosin (H&E), alcian blue.

### **6.3 Magnetic Resonance Imaging (MRI) Analysis**

MRI (GE SIGNA Creator 1.5T, Boston, Massachusetts, USA) scanning was performed post-operatively at 2, 4, and 8 months to monitor changes in joint fluid caused by inflammation. Joint effusion was identified on T2W images where synovial fluid appears hyperintense. In addition, other abnormal images of arthritis such as abnormal surface and structure of cartilage, endochondral ossification, abnormal shape of subchondral bone were evaluated by doctor of veterinary medicine, radiologist.

## **7. Statistical Analysis**

The statistical analysis was performed using GraphPad Prism 5.0 (Graphpad, San Diego, CA, USA). The significance of the data was confirmed with two-way ANOVA test followed by Bonferroni's correction.

# Result

## 1. Gross Appearance of Trochlear Block Recession Area in Each Group

Tissue samples were acquired at 8 months after surgery (**Figure 1**). The surgical area of articular surface in control group was not smoothly connected to normal tissue. Similar to the control group, LCCM + fibrin glue, fibrin glue, and syringe groups also showed no smooth fusion between the surgical area and normal tissue that makes gaps and redness. In contrast, in the case of LCCM + MAT + fibrin glue group, smooth fusion of the surgical area and normal tissue was observed, and redness was not confirmed. In addition, the surgical area of LCCM + MAT + fibrin glue group was filled with whitish tissue like normal articular cartilage than other groups.

Gross Appearance				
				
Control	LCCM + MAT + fibrin glue	LCCM + fibrin glue	Fibrin glue	Syringe

**Figure 1.** Gross appearance of trochlear block recession area.

## **2. Serum Level of Matrix Metalloproteinases-3 (MMP-3) and Tissue Inhibitors of Matrix Metalloproteinases-1 (TIMP-1)**

Synovial fluid MMP-3 and TIMP-1 were analyzed to observe the degree of inflammation response. Referring to **figure 2B**, during the postoperative period, the MMP-3 level was continuously confirmed to be lower in LCCM + MAT + fibrin glue groups and LCCM + fibrin glue groups compared to the control groups. In the case of fibrin glue groups, the MMP-3 level was very similar to that of LCCM + MAT + fibrin glue groups and LCCM + fibrin glue groups for the 2 months, but later rose and remained high to a level similar to that of the control groups. In the case of the syringe groups, on the contrary, the MMP-3 level was similar to that of the control group for the 2 months but later decreased to be similar to that of LCCM + MAT + fibrin glue groups and LCCM + fibrin glue groups. As shown in **figure 2A**, in the 2 months, the TIMP-1 level of LCCM + MAT + fibrin glue groups is slightly lower, but there is no significant difference compared to the control groups. After then, LCCM + MAT + fibrin glue groups had increased dramatically, showing a significant difference compared to any other groups in 8 months, but the control groups and fibrin glue groups showed a similar tendency. In the case of the LCCM + fibrin glue group and the syringe group, there was no dramatic increase in TIMP-1 level as in LCCM + MAT + fibrin glue group, but it continuously rises and remain higher than in the control group and fibrin glue group.

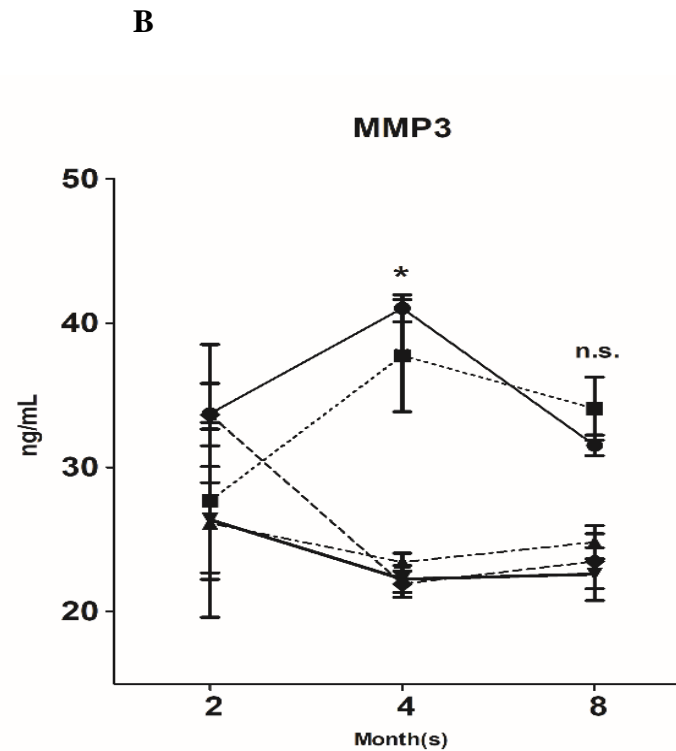
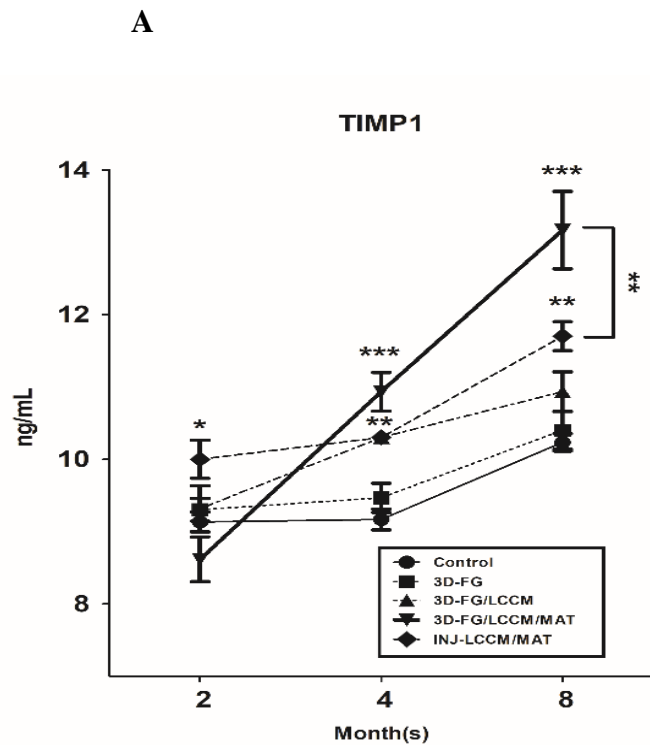


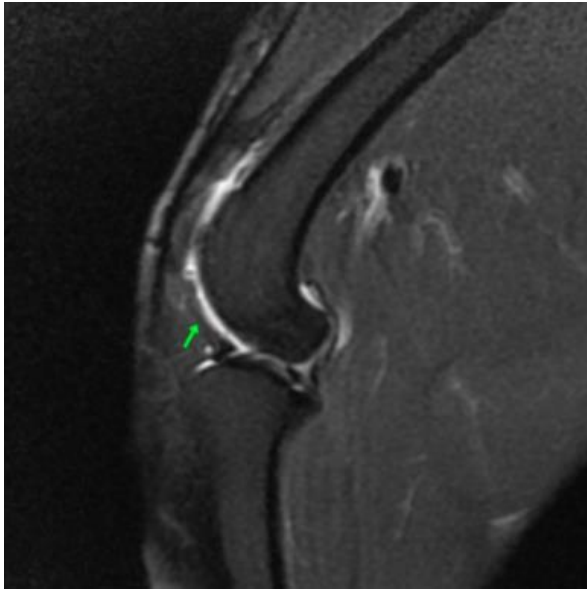
**Figure 2.** Enzyme-linked immunosorbent assay (ELISA) of TIMP-1 (A) and MMP-3 (B) expression in synovial joint.

\*  $p < 0.05$ , \*\*  $p < 0.01$ , \*\*\*  $p < 0.001$ , n.s.= not significant

### **3. Magnetic Resonance Imaging (MRI) Analysis**

MRI scanning was performed post-operatively at 8, 16, and 32 weeks to monitor changes in the joint fluid caused by inflammation. The stifle joint is a complex structure with various tissue types and MRI is suitable for evaluating the joint using different image planes and sequences. Synovial fluid and edema show high-signal intensity in T2-weighted sequences. In contrast, cortical bone, tendons, ligaments, and menisci are low-signal intensity because they are not naturally hydrated tissues (Marino & Loughin, 2010). As shown in figure 2, in control groups, joint effusion showing high signal intensity was observed more than in the LCCM + MAT + fibrin glue groups. There was no significant difference in joint fluid in other groups. There were no significant changes such as abnormal surface and structure of cartilage, endochondral ossification, or abnormal shape of subchondral bone in all groups (**Figure 3**).

**Control**



**LCCM + MAT + fibrin glue**

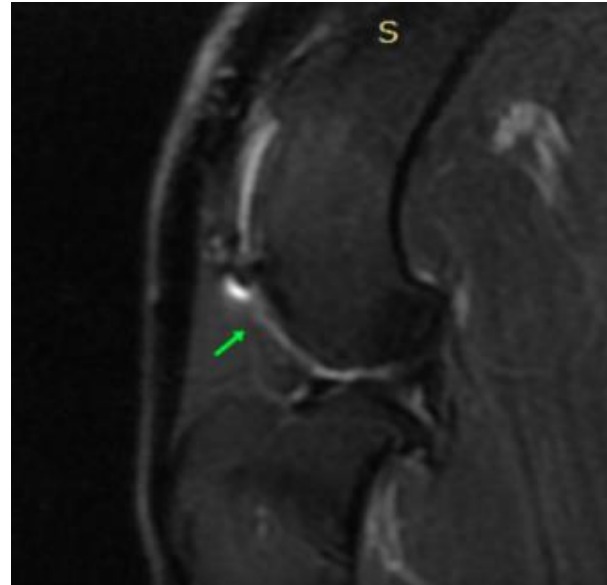


**Figure 3.** Assessment of knee articular cartilage using magnetic resonance imaging.

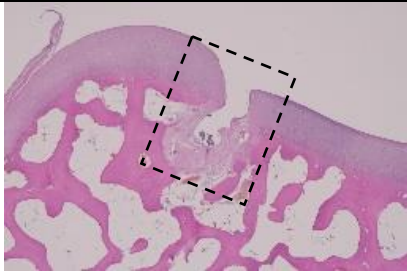
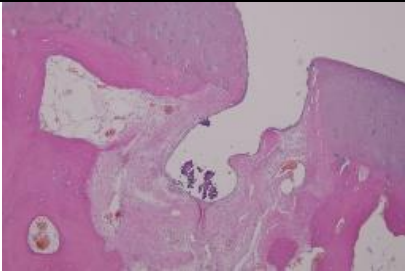
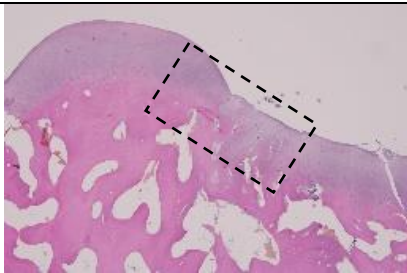
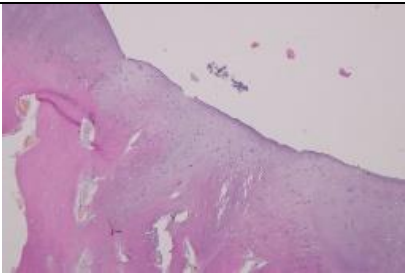
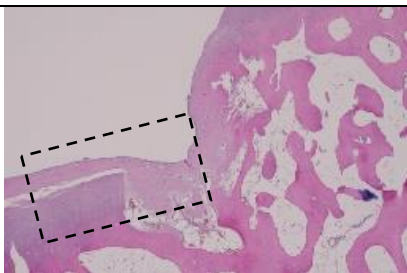
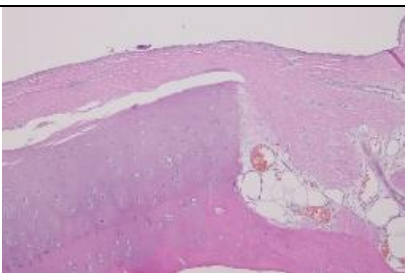
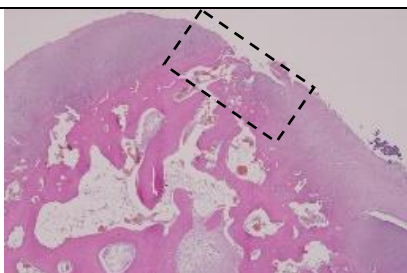
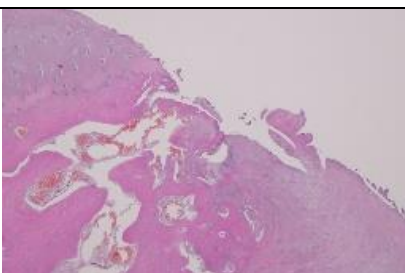
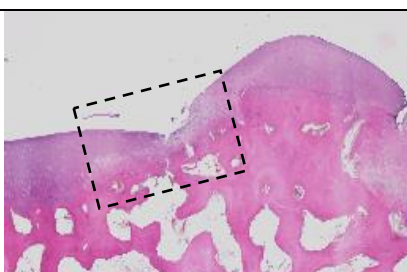
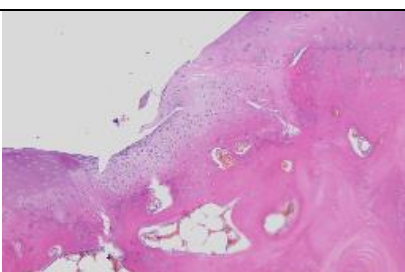
: Note that green arrows indicate joint effusion. More joint effusion was observed in the control groups than the LCCM + MAT + fibrin glue groups

## **4. Microscopic findings**

Microscopic examination was conducted with hematoxylin and eosin (H&E) and alcian blue staining knee articular cartilage tissue after euthanasia.

### **4.1. Microscopic Examination of Hematoxylin and Eosin (H&E)**

The control group indicated that the articular surface was discontinuous, consisting of fibrocartilage, fewer chondrocyte, and insufficient repair of lesion depth. In contrast, in the case of the LCCM + MAT + fibrin glue group, the articular cartilage surface was smooth, and continuous consisting of a hyaline and fibrocartilage mixture, denser chondrocyte distribution. In the case of the LCCM + fibrin glue group, although the articular surface was relatively continuous compared to the control group, the structure of the tissue was consisting of fibrocartilage and lower dense of chondrocyte compared to LCCM + MAT + fibrin glue group. The fibrin glue group showed discontinuous and poor lesion repair. In the case of the syringe group, the articular surface was less smooth compared to that of the LCCM + MAT + fibrin glue group, but relatively smooth compared to other groups. Interestingly, even in the syringe type group, there was denser chondrocyte distribution and hyaline and fibrocartilage mixture (**Figure 4**).

Group	40X	100X
Control		
LCCM + MAT + fibrin glue		
LCCM + fibrin glue		
Fibrin glue		
Syringe type		

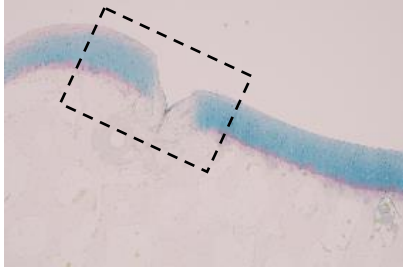
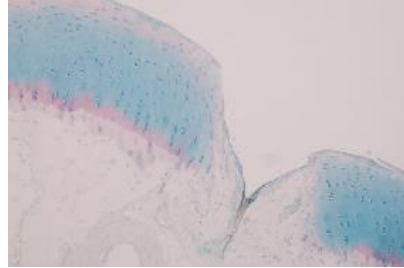
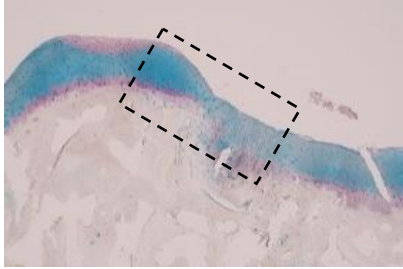
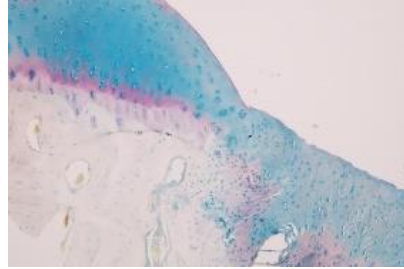
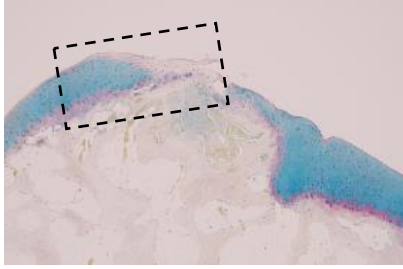
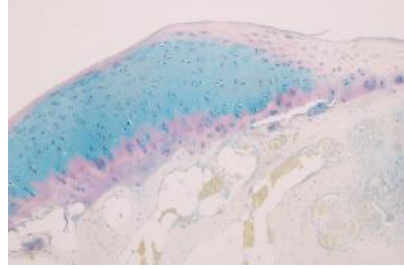
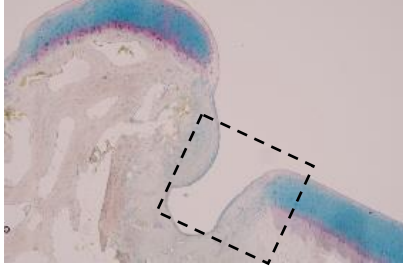
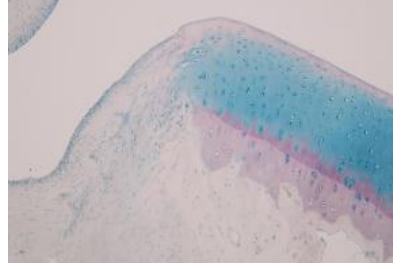
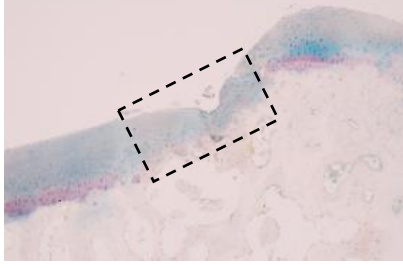
**Figure 4.** Hematoxylin and eosin (H&E) staining analysis of knee articular cartilage.

Representative hematoxylin and eosin (H&E) stained images of cartilage in each group. Compared to other group, LCCM + MAT + fibrin glue group has excellent integrity between lesion and normal tissue and denser cell distribution.

Black dotted rectangle: lesion area; low magnification view (40X) of the area within the rectangle in the right view (100X)

## **4.2. Alcian blue staining**

Alcian blue staining was conducted to investigate the characteristics of the newly formed tissue. Compared to other groups, the LCCM + MAT + fibrin glue group stained strongly with alcian blue in the newly formed tissue of the lesion area. This indicates that newly formed tissue of the LCCM + MAT + fibrin glue group are consisting of cartilage-like tissue containing sulfated GAGs. In the case of syringe type, alcian blue stain of newly formed tissue was less than LCCM + MAT + fibrin glue group, but relatively strong compared to other groups. There are no significant findings in other groups (**Figure 5**).

Group	40X	100X
<b>Control</b>		
<b>LCCM + MAT + fibrin glue</b>		
<b>LCCM + fibrin glue</b>		
<b>Fibrin glue</b>		
<b>Syringe type</b>		

**Figure 5.** Alcian blue staining analysis of knee articular cartilage.

Representative alcian blue stained images of cartilage in each group. Note that strongly stain in LCCM + MAT + fibrin glue group compared to the other groups.

Black dotted rectangle: lesion area; low magnification view (40X) of the area within the rectangle in the right view (100X).

## Discussion

In this study, we investigate the inflammatory alleviation and therapeutic effects of the osteochondral lesion by applying 3D printed biomatrix of allografted lyophilized costal cartilage matrix (LCCM), micronized adipose tissue (MAT), and fibrin glue using a canine trochlear block recession model. We propose a novel treatment with inflammatory alleviation and articular cartilage regeneration similar to normal tissue by applying a 3D printed biomatrix containing LCCM, MAT, and fibrin glue.

Adipose tissue is available in large quantities and can be acquired in a relatively less invasive procedure, so it is highly valuable as a biomaterial. The process of obtaining mesenchymal stem cells (MSCs) from adipose tissue such as suspension is complicated and regulated, but using MAT is a groundbreaking method in that it is very easy to be made and regeneration capacity can be taken. The mechanism of how MAT acts in regeneration cartilage is not yet fully understood. But, the high functional MSCs with chondrogenic differentiation capacity of adipose tissue is the main hypothesis, and in addition, various cytokines such as growth factors in adipose tissue seem to regulate the microenvironment (Bosetti et al., 2016; Louis et al., 2021; Tremolada et al., 2016).

In the field of research applying biomaterials to cartilage regeneration, the chondroinductivity of devitalized cartilage matrix (DVC) such as LCCM is emerging, because decellularized cartilage matrix processes limit chondroinductivity. However, even with DVC, the dense cartilage matrix still

suppresses cell infiltration and nutrient diffusion. Therefore, it is known that the cartilage regeneration effect is greater when applied with other biomaterials containing cytokines such as the growth factor (Kiyotake et al., 2016; Ryu et al., 2022). The study on the therapeutic effect of applying MAT to the articular joint lesion in dogs has not been studied. Also, there has been no study to compare when LCCM was used only and when applied with MAT.

In the case of the LCCM + MAT + fibrin glue group, H&E staining tests indicated more dense cell distribution, consisting of hyaline and fibrocartilage mixture, smooth surface, and integrity. In other groups, the articular surface was not smooth and the lower integrity. Except for the syringe type, in the other groups, the regeneration of cartilage lesions is mostly repaired by fibrous cartilage tissue. In alcian blue staining, the LCCM + MAT + fibrin glue group was strongly stained and also syringe group was relatively strongly stained compared to that of other groups. From these findings, it seems that LCCM and MAT combination repair by regenerating more high-intensity hyaline-like cartilage rather than fibrocartilage. Considering the previous studies and this study's results, MAT is considered to act as a bio-scaffold and regeneration factor. In addition, when LCCM and MAT are applied together, the regeneration effect looks greater. Histological assessments demonstrated LCCM + MAT + fibrin glue group had a better cartilage repair effect than the other groups. It is considered that LCCM and MAT show complementarily synergy effects of treatment.

The long-lasting anti-inflammatory activity of micro fragmented adipose tissue has been studied in vitro. The anti-inflammatory mechanism of MAT is a very complex phenomenon and is likely to be influenced by the combination of

molecules and extracellular vesicles released from MSCs (Nava et al., 2019). In this study, the MMP-3 level of LCCM + MAT + fibrin glue, LCCM + fibrin glue, and syringe group was lower than the control group at 4 and 8 months, in addition, the TIMP-1 level was higher. On the other hand, in the case of the fibrin group, there is a similar MMP-3 and TIMP-1 level tendency to the control group, which means that only the application of fibrin glue does not affect inflammation alleviation, and the application of LCCM or MAT help reduce inflammation. Especially, the LCCM + MAT + fibrin glue group, containing all biomaterials, confirmed a dramatic increase in TIMP-1 level and the lowest MMP-3 level. In addition, MRI showed joint fluid elevation in the control groups compared to the LCCM + MAT + fibrin glue group. Put these findings together, we found that applying a combination of LCCM with MAT has a long-lasting anti-inflammatory effect in vivo. It is meaningful to confirm the therapeutic effect using actual disease models.

Traditional cartilage regeneration techniques and studies have adopted the manual dispensing methods in applying biomaterials. However, in this study, biomaterials were constructed and applied by 3D printing technique. Compared to the 3D-printed LCCM + MAT + fibrin glue and syringe group, the syringe group had less inflammation alleviation and cartilage regeneration effect. The two groups have the same type of biomaterial, but there is a difference in the applied form. The biggest difference between the two groups due to applied form is the degree of contact with the lesion. In the syringe type group, it seemed to lack stability and contact with lesion in the process of applying syringe type biomaterials. This means that the greater the degree of contact with the patient's lesion, the greater the

therapeutic effect. By applying 3D printing technique, it was confirmed that a greater therapeutic effect can be expected by increasing the degree of contact through the size and shape of the implant and the appropriate placement of biomaterials. Previously we demonstrated that three-dimensional printed biomaterials containing LCCM and MAT derived from xenogenic human origin could repair osteochondral lesions and alleviate inflammation in canine osteochondral defect models.(12) In general, allograft biomaterial implant has the advantage of being relatively safer and less risk of rejection than xenograft. There had been no studies on the application of allograft MAT to cartilage lesions in canine models, and this study demonstrated its therapeutic effect and safety without any side effects. There are several limitations to this experiment. One of the limitations is the absence of a placebo group. In addition, if the physical and biological properties of biomaterial ink can be improved to make it more stable and close contact, it is believed that there will be a greater therapeutic effect.

## **Conclusion**

We confirmed that cartilage was regenerated using a 3D-printed allogenic biomaterial implant containing LCCM and MAT in the canine trochlear block recession model. Based on this study, it is considered that it will be more effective to manufacture and apply the biomaterial implant combining LCCM and MAT to repair cartilage lesions in dogs.

## References

- Armiento, A. R., Alini, M., & Stoddart, M. J. (2019). Articular fibrocartilage - Why does hyaline cartilage fail to repair? *Advanced Drug Delivery Reviews*, *146*, 289–305.
- Bosetti, M., Borrone, A., Follenzi, A., Messaggio, F., Tremolada, C., & Cannas, M. (2016). Human lipoaspirate as autologous injectable active scaffold for one-step repair of cartilage defects. *Cell Transplantation*, *25*(6), 1043–1056.
- Di Dona, F., della Valle, G., & Fatone, G. (2018). Patellar luxation in dogs. *Veterinary Medicine: Research and Reports*, *Volume 9*, 23–32.
- DiVincenzo, M. J., Frydman, G. H., Kowaleski, M. P., Vanderburg, C. R., Lai, B., Oura, T. J., & Jennings, S. H. (2017). Metallosis in a Dog as a Long-Term Complication Following Total Hip Arthroplasty. *Veterinary Pathology*, *54*(5), 828–831.
- Dokic, Z., Lorinson, D., Weigel, J. P., & Vezzoni, A. (2015). Patellar groove replacement in patellar Luxation with severe femoro-patellar osteoarthritis. *Veterinary and Comparative Orthopaedics and Traumatology*, *28*(2), 124–130.

- Dzobo, K., Motaung, K. S. C. M., & Adesida, A. (2019). Recent trends in decellularized extracellular matrix bioinks for 3D printing: An updated review. In *International Journal of Molecular Sciences* (Vol. 20, Issue 18). MDPI AG.
- Escobar Ivirico, J. L., Bhattacharjee, M., Kuyinu, E., Nair, L. S., & Laurencin, C. T. (2017). Regenerative Engineering for Knee Osteoarthritis Treatment: Biomaterials and Cell-Based Technologies. *Engineering*, 3(1), 16–27.
- Falah, M., Nierenberg, G., Soudry, M., Hayden, M., & Volpin, G. (2010). *Treatment of articular cartilage lesions of the knee*. 621–630.
- Journal, T. (1988). *Stress Fractures of the Knee than has*. 70(5).
- Kiyotake, E. A., Beck, E. C., & Detamore, M. S. (2016). Cartilage extracellular matrix as a biomaterial for cartilage regeneration. *Annals of the New York Academy of Sciences*, 1383(1), 139–159.
- Knutsen, G., Isaksen, V., Johansen, O., Engebretsen, L., Ludvigsen, T. C., Drogset, J. O., Grøntvedt, T., Solheim, E., Strand, T., & Roberts, S. (2004). Autologous Chondrocyte Implantation Compared with Microfracture in the Knee: A Randomized Trial. *Journal of Bone and Joint Surgery - Series A*, 86(3), 455–464.
- Louis, M. L., Dumonceau, R. G., Jouve, E., Cohen, M., Djouri, R., Richardet, N.,

Jourdan, E., Giraud, L., Dumoulin, C., Grimaud, F., George, F. D., Veran, J., Sabatier, F., & Magalon, J. (2021). Intra-Articular Injection of Autologous Microfat and Platelet-Rich Plasma in the Treatment of Knee Osteoarthritis: A Double-Blind Randomized Comparative Study. *Arthroscopy - Journal of Arthroscopic and Related Surgery*, 37(10), 3125-3137.e3.

Marcacci, M., Filardo, G., & Kon, E. (2013). Treatment of cartilage lesions: What works and why? In *Int. J. Care Injured* (Vol. 44).

Marino, D. J., & Loughin, C. A. (2010). Diagnostic imaging of the canine stifle: A review. *Veterinary Surgery*, 39(3), 284–295.

Nava, S., Sordi, V., Pascucci, L., Tremolada, C., Ciusani, E., Zeira, O., Cadei, M., Soldati, G., Pessina, A., Parati, E., Slevin, M., & Alessandri, G. (2019). Long-Lasting Anti-Inflammatory Activity of Human Microfragmented Adipose Tissue. *Stem Cells International*, 2019.

Romesburg, J. W., Wasserman, P. L., & Schoppe, C. H. (2010). Metallosis and Metal-induced synovitis following total knee arthroplasty: Review of Radiographic and CT Findings. *Journal of Radiology Case Reports*, 4(9), 7–17.

Ryu, J., Brittberg, M., Nam, B., Chae, J., Kim, M., Colon, Y. I., Magneli, M., Takahashi, E., Khurana, B., & Bragdon, C. R. (2022). Evaluation of Three-

Dimensional Bioprinted Human Cartilage Powder Combined with Micronized Subcutaneous Adipose Tissues for the Repair of Osteochondral Defects in Beagle Dogs. *International Journal of Molecular Sciences*, 23(5), 1–14.

Sasaki, A., Mizuno, M., Mochizuki, M., & Sekiya, I. (2019). Mesenchymal stem cells for cartilage regeneration in dogs. *World Journal of Stem Cells*, 11(5), 254–269.

Spencer Johnston, E. A., James, D., Waggoner Professor Head, M., Tobias, K. M., & Professor, D. (n.d.). *Veterinary Surgery SMALL ANIMAL SECOND EDITION Marc Kent, DVM, DACVIM (Small Animal Internal)*.

Sutherland, A. J., Converse, G. L., Hopkins, R. A., & Detamore, M. S. (2015). The bioactivity of cartilage extracellular matrix in articular cartilage regeneration. *Advanced Healthcare Materials*, 4(1), 29–39.

Tremolada, C., Colombo, V., & Ventura, C. (2016). Adipose Tissue and Mesenchymal Stem Cells: State of the Art and Lipogems® Technology Development. In *Current Stem Cell Reports* (Vol. 2, Issue 3, pp. 304–312). Springer International Publishing.

Yoon, D. Y., Kang, B. J., Kim, Y., Lee, S. H., Rhew, D., Kim, W. H., & Kweon, O. K. (2015). Degenerative joint disease after medial patellar luxation repair in

dogs with or without trochleoplasty. *Journal of Veterinary Clinics*, 32(1), 22–27.

# 국문 초록

## 개의 활차 블록 절제 모델에서 관절 재생을 위한 3D 프린터로 제작된 동중유래 생체재료 이식의 효과 연구

지도교수 김 민 수

이 한 솔

서울대학교 대학원

수의학과 임상수의학 전공

본 연구의 목적은 동중유래 동결건조 갈비뼈 연골 분말 (LCCM), 미세화 지방조직 (MAT) 및 피브린 접착제 (fibrin glue)를 포함하여 3D 프린터로 제작한 생체재료의 염증감소 및 치료효과를 확인하는 것이다. 본 연구에서는 개의 활차 블록 절제 모델을 사용하였다. 대조군은 오직 활차 블록 절제만 적용하였으며 실험군은 생체 이식물의 구성에 따라 LCCM + MAT + fibrin glue, LCCM + fibrin glue, fibrin glue와 syringe 형태 그룹으로 분류하였다. 치료효과를 증명하기 위해 자기공명영상 (MRI), 관절액의 효소면역측정법 (ELISA) 및 조직병리 검사를 진행하였다. 관절연골의 효

소면역측정법상에서 LCCM + MAT + fibrin glue 그룹이 matrix metalloproteinase-3 (MMP-3) 수치가 감소하고 tissue inhibitor of metalloproteinase-1 (TIMP-1) 수치가 증가하는 경향을 보였다. 또한, 자기공명영상 분석상에서 LCCM + MAT + fibrin glue 그룹보다 대조군에서 관절액이 상승한 것을 확인하였다. 따라서, LCCM + MAT + fibrin glue 그룹이 다른 그룹들과 비교하여 관절 염증과 관절염으로 인한 관절액이 적은 것으로 생각된다. 조직병리검사상에서 LCCM + MAT + fibrin glue 그룹이 다른 그룹들과 비교하여 정상조직과 병변 사이의 완전성, 연골세포 수, 유리연골의 재생이 우월함을 보여주었다. 우리는 LCCM + MAT + fibrin glue 그룹에서 연골 손상의 치료 효과가 높은 것을 확인하였다. 실험적으로 유발된 개의 연골 병변에서 3D 프린터로 제작된 LCCM + MAT + fibrin glue 생체재료가 연골수복, 재생 및 염증감소 효과에 훌륭한 치료효과가 있는 것을 입증하였다.

---

**주요어:** 관절 연골, 3D 프린트 제작 이식물, 재생, 개의 무릎, 활차 블록 절제

**학번:** 2020-28574